Original Article

Therapeutic effect of Xue Niao An on glyoxylate-induced calcium oxalate crystal deposition based on urinary metabonomics approach

Zhongjiang Peng,[1,†] Wei Chen,[1,†] Songyan Gao,[2] Li Su,[2] Na Li,[2] Li Wang,[1] Ziyang Lou,[2] Xin Dong[2,*] and Zhiyong Guo[1,*]

[1]Department of Nephrology, Changhai Hospital and [2]School of Pharmacy, Second Military Medical University, Shanghai 200433, China

(Received 6 May, 2014; Accepted 3 July, 2014; Published online 4 October, 2014)

The anti-nephrolithiasis effect of Xue Niao An (XNA) capsules is explored by analyzing urine metabolic profiles in mouse models, with ultra-high performance liquid chromatography quadrupole time-of-flight mass spectrometry (UPLC-Q-TOF/MS). An animal model of calcium oxalate crystal renal deposition was established in mice by intra-abdominal injection of glyoxylate. Then, treatment with XNA by intra-gastric administration was performed. At the end of the study, calcium deposition in kidney was measured by Von Kossa staining under light microscopy, and the Von Kossa staining changes showed that XNA significantly alleviated the calcium oxalate crystal deposition. Meanwhile, urine samples for fifteen metabolites, including amino acids and fatty acids, with significant differences were detected in the calcium oxalate group, while XNA treatment attenuated metabolic imbalances. Our study indicated that the metabonomic strategy provided comprehensive insight on the metabolic response to XNA treatment of rodent renal calcium oxalate deposition.

***Key Words*: metabonomics, Xue Niao An, calcium oxalate, UPLC-Q-TOF/MS**

In last few decades, the increased occurrence of urolithiasis has become a key global health issue.[1,2] Recent epidemic studies have found that kidney stone formation was associated with multiple metabolic dysfunctions, such as hypertension, diabetes and obesity.[3] Furthermore, some research indicated that patient history of kidney stones would be an independent risk factor of chronic kidney disease (CKD), end stage renal disease (ESRD) and cardiovascular disease.[4–7] As a systematic evaluation of endogenous metabolites, metabonomics had been applied in research of metabolic diseases and natural products effects.[8–9] Thus, mass spectrometric-based metabonomics research would be an option to explore etiology and therapeutic strategy.

Due to the widespread incidence of kidney stones, especially in the tropical and subtropical zone, many herbal remedies, including *Desmodium styracifolium*, *Pyrrosiae petiolosa*, *Rosa canina*, and apocynin have been used for the prevention and treatment of kidney stones.[10,11] Being traditional Chinese medicine (TCM), the Xue Niao An (XNA) capsule consists of *Clerodendranthus spicatus*, *Cirsium setosum*, *Rhizoma imperatae*, and *Cortex Phellodendri* (Chinese Drug Standards: 2002ZD-0793). The most important component is *Clerodendranthus spicatus*, a popular folk medicine (also known as "Shen Cha" in Chinese), which is widely distributed in southern China and southeast Asia and has been used for the treatment of urolithiasis, nephritis and rheumatism for hundreds of years.[12,13] However, little is known of the exact mechanism of XNA in urolithiasis treatment, especially from the aspect of metabolite abnormality. In the present study, a urinary metabonomics-based study was conducted to investigate the potential effects of XNA in an animal model of urolithiasis, which is characterized by renal calcium oxalate (CaOx) deposition.

Materials and Methods

Chemicals and reagents. Methanol and acetonitrile were purchased from Merck (Darmstadt, Germany). Formic acid was obtained from Fluka (Buchs, Switzerland). Ultrapure water was prepared using a Milli-Q water purification system (Millipore Corp, Billerica, MA). Glyoxylate (TCI, Tokyo, Japan), Von Kossa staining commercial kit (Shunbai, Shanghai, China) and Xue Niao An (Yunnan Lixiang Pharmaceutical Co., Ltd., Z20026104) were obtained from local distributors. Other chemicals were of analytical grade.

Animal experiment and sample collection. Animal studies followed the recommendations of the NIH Guide for the Care and Use of Laboratory Animals. Eighteen wild type male C57BL/6 mice (7–8 weeks old) were purchased from the Shanghai SLAC Lab Animal Co., Ltd. (Shanghai, China) and kept in an animal facility of the Second Military Medical University (Shanghai, China). All mice had free access to drinking water (*ad libitum*) and regular chow every day and were kept under a controlled 12 h light/dark cycle at 20–25°C with the relative humidity at 55–65%. After conditioned housing for one week, 18 mice were equally divided into the following three groups of 6 mice each: the control, the CaOx, and XNA-treated groups. Except for the control group, all mice were administered glyoxylate (100 mg/kg/day) by daily intra-abdominal injection for 5 consecutive days. The administration method used in this study was optimized by preliminary experiments according to Okada *et al.*,[14] the control group was intra-abdominally injected daily with normal volume saline (20 ml/kg/day) for 5 consecutive days, the XNA-treated group was given 5 g/kg/day of an aqueous extract of XNA by gavage in addition to glyoxylate injection for 5 days. Twenty four-hour urine was collected on day 5 after the administration of glyoxalate.

Urine sample preparation. Prior to analysis, a 100 μl aliquot of urine sample was mixed with 300 μl of acetonitrile and vortexed to precipitate the proteins. After centrifugation at 13,000 rpm for 15 min at 4°C, the clear supernatant was transferred to the sampling vial, and an aliquot of 3 μl was injected for metabonomics analysis.

Biochemistry and histological analysis. The levels of calcium, phosphate, magnesium and creatinine in urine were measured by a BC-2800 Vet animal auto biochemistry analyzer (Shihai, Guangdong, China). The apical portions of the kidney

*To whom correspondence should be addressed.
E-mail: dongxinsmmu@126.com (Xin Dong),
drguozhiyong@163.com (Zhiyong Guo)
†These authors contributed equally to this work.

doi: 10.3164/jcbn.14-61

were fixed in the 4% buffered formalin and embedded in paraffin wax. Slices with 3 μm thickness were prepared for Von Kossa staining, and semi-quantitative analysis was performed by 20 random views with 400× magnification.

UPLC-Q-TOF/MS analysis. UPLC-Q-TOF/MS analysis was performed on an Agilent 1290 Infinity LC system equipped with an Agilent 6530 Accurate-Mass Quadrupole Time-of-Flight (Q-TOF) mass spectrometer (Agilent Technologies, CA). Chromatographic separations were performed at 40°C on an ACQUITY UPLC HSS T3 column (2.1 mm × 100 mm, 1.8 μm, Waters, Milford, MA). The mobile phase consisted of 0.1% formic acid (A) and acetonitrile modified with 0.1% formic acid (B). The optimized UPLC elution conditions were 0–2 min, 5% B; 2–10 min, 5–15% B; 10–14 min, 15–30% B; 14–17 min, 30–95% B; 17–19 min, 95% B, and the post time was set to 6 min for equilibrating the system. The flow rate was set to 0.4 ml/min and the injection volume was 3 μl. The auto-sampler was maintained at 4°C. An electrospray ionization source (ESI) was used both in positive mode and negative mode. The optimized conditions were as follows: capillary voltage, 4 kV for positive mode and 3.5 kV for negative mode; drying gas flow, 11 L/min; gas temperature, 350°C; nebulizer pressure, 45 psig. fragmentor voltage, 120 V; skimmer voltage, 60 V. Data were collected in centroid mode from 50 to 1,100 m/z. Potential biomarkers were further analyzed by MS/MS, the collision energy was set to 10–50 eV.

Data processing. Each sample was represented in a total ion current (TIC) chromatogram. The UPLC–MS raw data were converted into a common data format (.mzData) files by the Agilent MassHunter Qualitative software, in which the isotope interferences were exclude, and the threshold was set to 0.1%. The program XCMS (http://metlin.scripps.edu/download/) was applied for peak detection, RT alignment and peak integration to generate a visual data matrix. The variables present in at least 80% of either group were extracted. To correct for the MS response shift, the data of each sample was normalized to total intensity, and then the three-dimensional data including RT m/z pair, sample name, and normalized ion intensity were imported to SIMCA-P software (Umetrics, Sweden) for principal component analysis (PCA) and partial least squares-discriminate analysis (PLS-DA). The heat map of the different metabolites was created online by the MetaboAnalyst platform (http://www.metaboanalyst.ca).

Statistical analysis. The biochemistry data were expressed as the mean ± SD. Statistically significant differences in mean values were tested by one-way ANOVA and the Tukey's post-hoc test in SPSS 17.0. The differences were considered significant when $p<0.05$.

Results

Histology and biochemistry. According to the staining of Von Kossa, the calcium deposition in XNA-treated mice kidney was much less than that from mice of the CaOx group. Representative images of Von Kossa staining are shown in Fig. 1A–C. Semi-quantitative analysis also found that the differences in positive staining area were significant (Fig. 1D). The significantly lower ratio of calcium and creatinine from urine in the XNA group compared to the CaOx group indicated the reno-protective effect of XNA, as well as a decreased ratio of phosphate and creatinine in the XNA group compared to in the CaOx group (Table 1).

Table 1. Ratios of the urine concentration of Ca, P and Mg to creatinine in Control, CaOx and XNA treated mice

	Ca/Creatinine	P/Creatinine	Mg/Creatinine
Control	0.30 ± 0.08	3.3 ± 1.1	0.14 ± 0.06
CaOx	0.58 ± 0.20*	7.4 ± 2.9*	0.18 ± 0.07
XNA	0.42 ± 0.12#	4.4 ± 1.9#	0.15 ± 0.08

*Vs control group $p<0.05$, #vs CaOx group $p<0.05$.

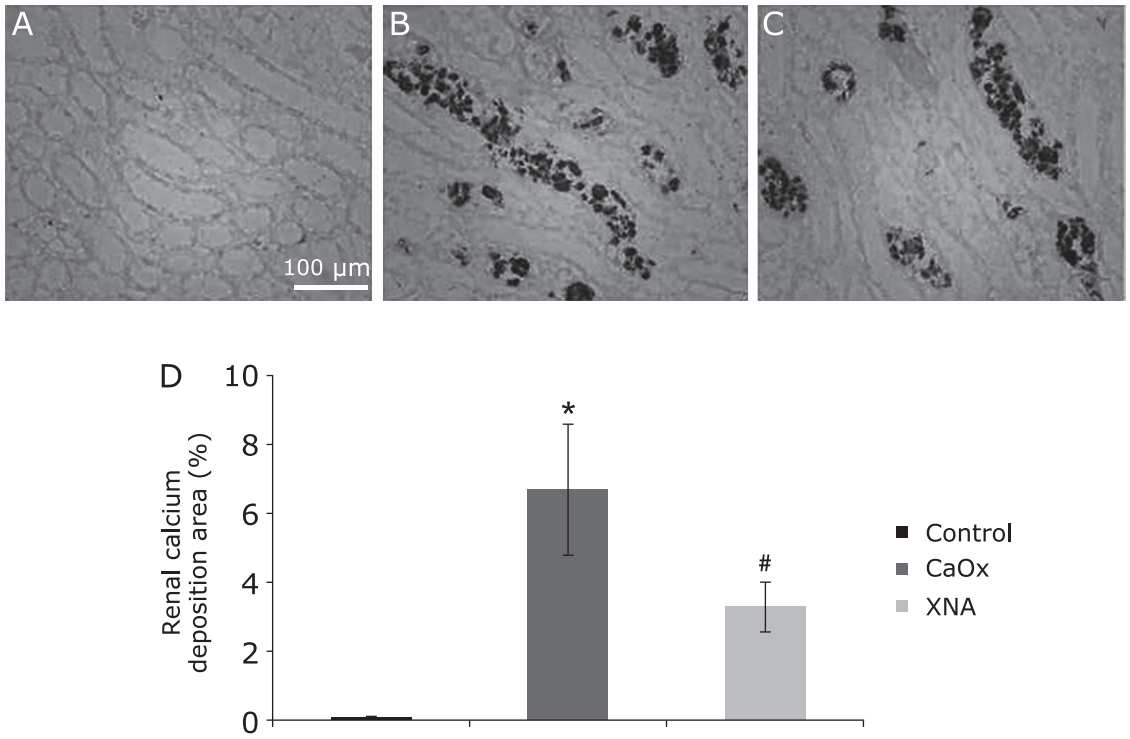

Fig. 1. Representative views of Von kossa staining for calcium deposition from the cortex and medulla junction of kidney. (A) control group; (B) CaOx group; (C) XNA group; (D) Semi-quantitative analysis of calcium deposition by the area of positive staining from every 20 random views. (*vs control group $p<0.05$, #vs CaOx group $p<0.05$)

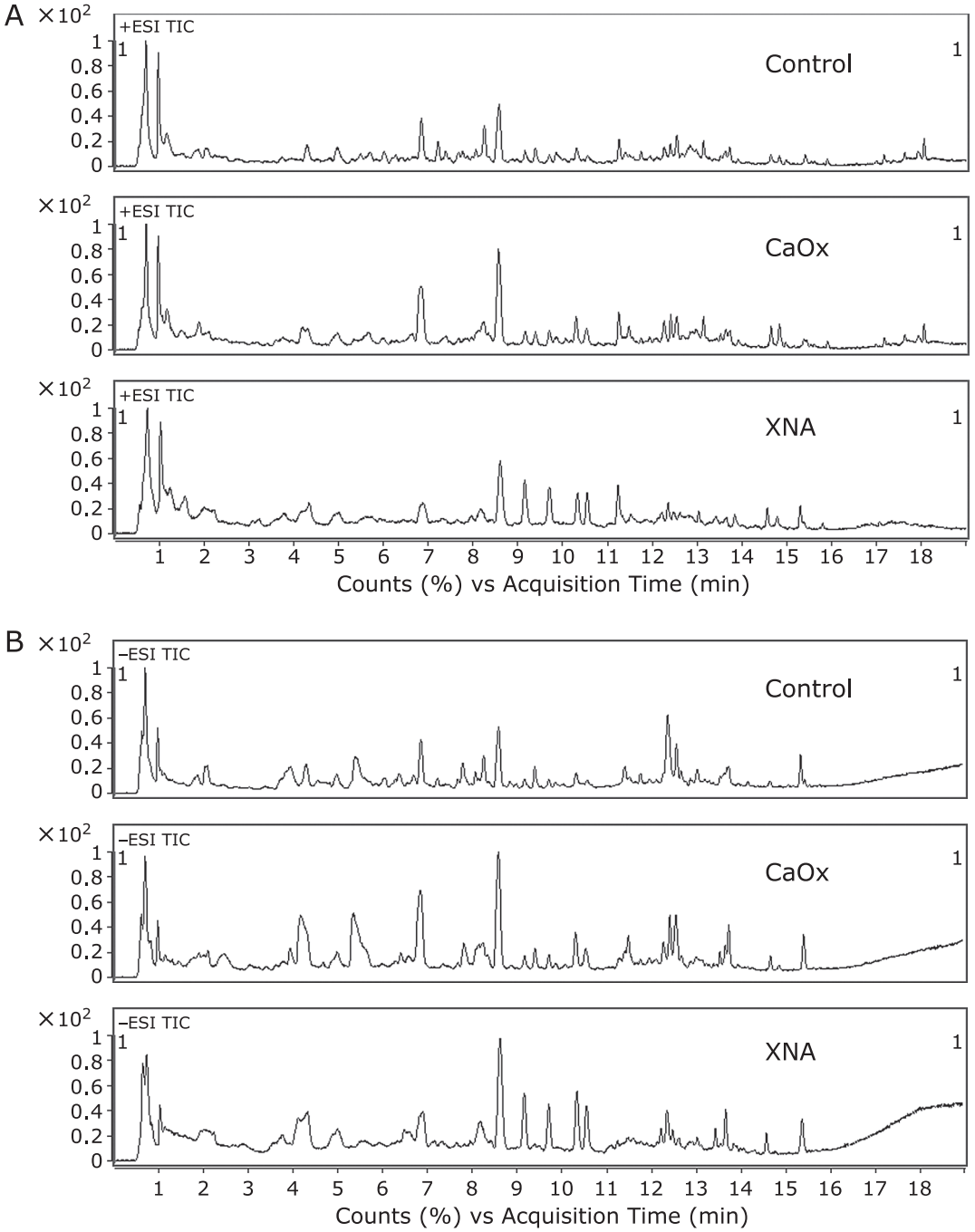

Fig. 2. Representative base peak chromatograms (BPC) obtained in ESI positive ion mode (A) and negative ion mode (B).

Discovery and identification of biomarkers. In the present research, the metabolic profiling analysis was performed in UPLC-Q-TOF/MS and represented the total ion chromatograms (TICs) obtained from the positive (Fig. 2A) and negative modes (Fig. 2B) in separated groups were illustrated. Two multivariate statistical analysis, PCA and PLS-DA, were conducted to visualize the metabolic shift. The score plots (Fig. 3A–D) showed CaOx and XNA groups were altered from the control group. The scatter plots (Fig. 3E and F) showed that the potential metabolites were selected and showed as the spots far away from origin of coordinates. The ions with variable importance values greater than 1.0 were considered to be important differential metabolites, then a one-way ANOVA and Tukey's post-hoc test were performed to assess statistical significance. Finally, there were 15 metabolites with significant differences between the control and CaOx group that were considered as potential biomarkers. During the metabonomics study, identifying different metabolites was an important and challenging task. The first step was to confirm the ions based on the extracted ion chromatogram (EIC). The second step was to input the exact masses of the quasi molecular ions into online databases, such as the Metlin database (http://metlin.scripps.edu/), Human Metabolome Database (http://www.hmdb.ca/), and Mass Bank (http://www.massbank.jp/), and search for the possible metabolites. The third step was to compare the MS/MS spectra

doi: 10.3164/jcbn.14-61

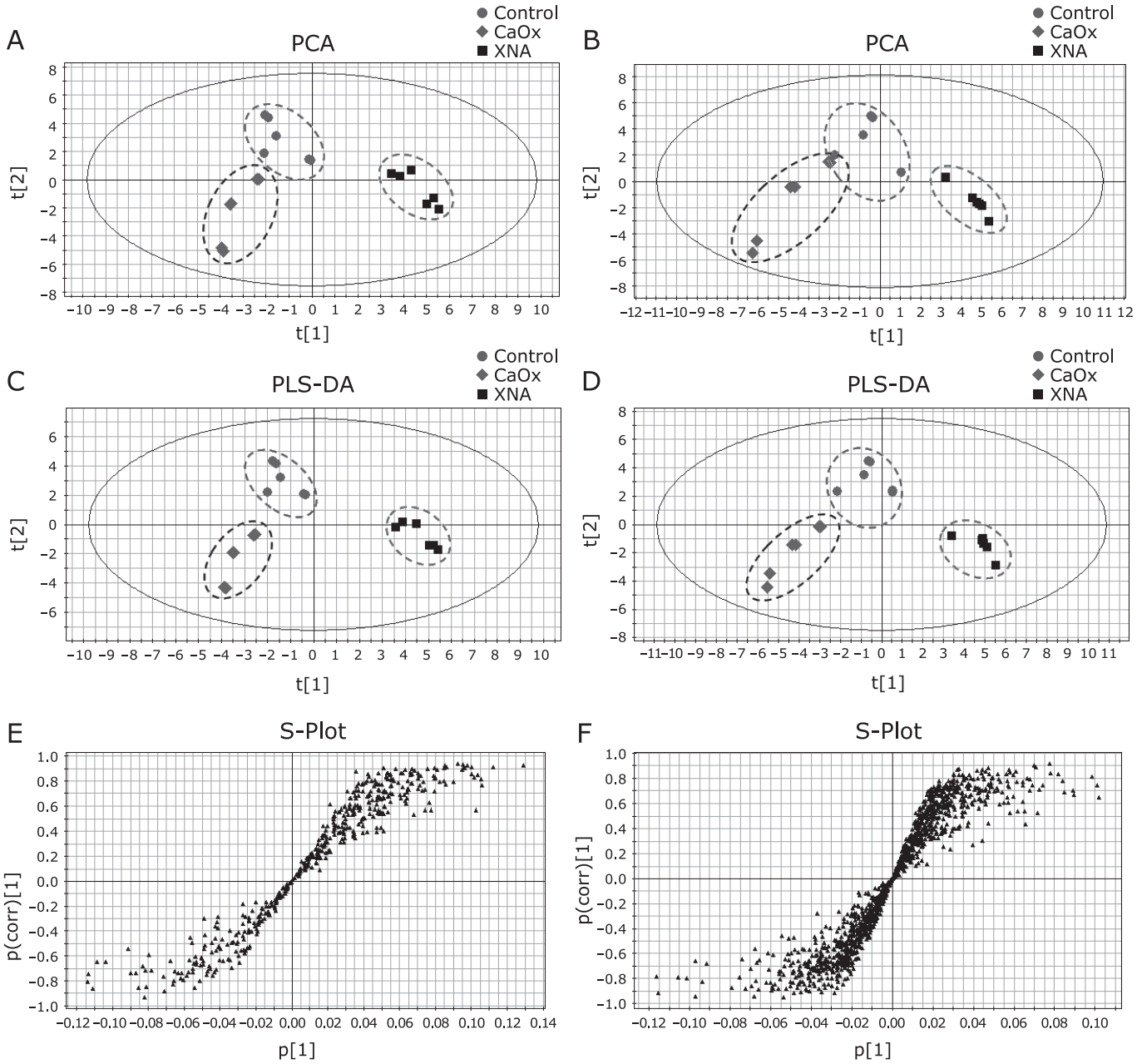

Fig. 3. Multivariate's statistical analysis derived from urinary different metabolites from Control group (■), CaOx group (●) and XNA group (◆). PCA score plot from ESI positive ion mode (A), negative ion mode (B); PLS-DA score plot from ESI positive ion mode (C), negative ion mode (D); S-plot based on PLS-DA analysis from ESI positive ion mode (E), negative ion mode (F).

with the MS/MS information from the above databases to verify the structure of putative metabolites. The fourth and final step was to confirm the identification of metabolites as biomarkers using standard samples based on the retention time and the fragments information.

Evaluation of the therapeutic mechanism of XNA on crystal-induced kidney injury. Fifteen urinary metabolites have been identified as potential biomarkers of renal CaOx deposition from the glyoxylate treatment of mice. Therefore, it was reasonable to use these fifteen metabolites as monitors to evaluate the protective effects of XNA. Table 2 provided the change trends for the different biomarkers in the XNA-treated mice. To more clearly characterize the therapeutic effects of XNA, a heatmap of the relative intensity changes of the 15 metabolites in the different groups is shown in Supplemental Fig. 1*. The related pathway of each biomarker is also shown in Table 2. These biomarkers are mainly related to amino metabolism, energy metabolism, and fatty acid metabolism. These pathways might play a key role in the protective effect of XNA in crystal induced kidney injury and the study of these pathways would be helpful to interpret the therapeutic mechanism.

Discussion

According to Okada's method, we have successfully replicated the deposition of calcium oxalate crystal in mouse kidney. Consistent with previous study, widespread tubular injury was found in the glyoxylate treated mice. In addition, the renal damage could

*See online. https://www.jstage.jst.go.jp/article/jcbn/55/3/55_14-61/_article/supplement

Table 2. Potential biomarkers related to glyoxylate-induced renal damage and the targeted metabolites of XNA involoved

NO.	t_R/min	m/z	Ion	Formula	Identification	[a]CaOx group		[b]XNA group		Related pathway
						p value	Trend	*p* value	Trend	
1	0.72	138.06	$[M + H]^+$	$C_7H_7NO_2$	p-Aminobenzoic acid	<0.001	↓	0.943	↑	Folic acid metabolism
2	1.04	139.05	$[M + H]^+$	$C_6H_6N_2O_2$	Urocanic acid	<0.001	↓	0.958	↓	Histidine metabolism
3	0.74	141.07	$[M + H]^+$	$C_6H_8N_2O_2$	1,3-Dimethyluracil	<0.001	↓	<0.001	↑	Purine metabolism
4	1.04	166.07	$[M + H]^+$	$C_6H_7N_5O$	7-Methylguanine	<0.001	↓	0.006	↑	Purine metabolism
5	2.46	188.09	$[M + H]^+$	$C_8H_{13}NO_4$	2-Keto-6-acetamidocaproate	<0.001	↓	0.162	↑	Lysine metabolism
6	8.42	203.13	$[M + H]^+$	$C_{10}H_{18}O_4$	Sebacic acid	<0.001	↑	<0.001	↓	Fatty acid metabolism
		225.11	$[M + Na]^+$							
		201.11	$[M - H]^-$							
7	4.5	206.04	$[M + H]^+$	$C_{10}H_7NO_4$	Xanthurenic acid	<0.001	↓	0.019	↑	Tryptophan metabolism
		204.03	$[M - H]^-$							
8	5.17	216.12	$[M + H]^+$	$C_{10}H_{17}NO_4$	Propenoylcarnitine	<0.001	↓	0.003	↑	Fatty acid metabolism
		214.11	$[M - H]^-$							
9	6.39	218.14	$[M + H]^+$	$C_{10}H_{19}NO_4$	Propionylcarnitine	<0.001	↓	0.086	↑	Fatty acid metabolism
10	11.43	220.14	$[M + H]^+$	$C_{10}H_{21}NO_2S$	Pentahomomethionine	0.038	↓	<0.001	↑	Methionine metabolism
11	2.99	234.13	$[M + H]^+$	$C_{10}H_{19}NO_5$	Hydroxypropionylcarnitine	0.047	↓	0.002	↑	Fatty acid metabolism
12	8.35	172.1	$[M - H]^-$	$C_8H_{15}NO_3$	Isovalerylalanine	0.017	↑	0.037	↓	Alanine metabolism
13	1.99	188.09	$[M - H]^-$	$C_7H_{15}N_3O_3$	Homocitrulline	<0.001	↓	0.195	↑	Lysine metabolism
14	9.91	217.11	$[M - H]^-$	$C_{10}H_{18}O_5$	3-Hydroxysebacic acid	0.03	↑	0.006	↓	Fatty acid metabolism
15	13.19	353.04	$[M + COO]^-$	$C_9H_{13}N_2O_8P$	dUMP	<0.001	↓	0.177	↑	Pyrimidine metabolism

[a]Compared to control group. [b]Compared to CaOx group. [c]dUMP: Deoxyuridine monophosphate (dUMP).

be alleviated by treatment with XNA. In recent years, several studies have highlighted the potential efficacy of complementary and alternative medicine for the prevention chemical related renal injury,[15] including the CaOx induced kidney damage. For example, Zuo *et al.*[16] demonstrated that the efficacy of apocynin treatment in reducing the production of reactive oxygen species (ROS) is associated with renal injury and crystal deposition in the kidneys of rats with hyperoxaluria. Another study reported that 1,2,3,4,6-penta-*O*-galloyl-beta-D-glucose, a water soluble gallotannin similar toepigallocatechin-3-gallate, reduced renal crystallization and oxidative renal cell injury and may be a candidate preventative agent for nephrolithiasis.[17] In the present study, the metabonomic changes of urine in the CaOx group and XNA-treated group mice were determined. The changes involved in amino acid metabolism, fatty acid metabolism and in other metabolism were integrated and are illustrated in Supplemental Fig. 2*.

Several studies showed that tryptophan metabolism was disrupted in kidney diseases.[18–20] Xanthurenic acid (XA) is a metabolite from tryptophan catabolism. It has been reported to be reduced in some models of renal injury, such as mercuric chloride and cyclosporin A.[21] Consistent with previous reports, there was a similar effect in our model. In conjunction with injury to tubular cells, XA decreased in the urine of the CaOx group, and increased in the XNA-treated group. It indicated that the tryptophan pathway was disturbed. In kidney, XA is transported by organic anion transporters 1 (OAT1) and organic anion transporters 3 (OAT3).[22] The function of organic anion transporters (OATs) expressed on the brush border and basolateral membrane of tubular cells of the kidney and belonging to the SLC22A family of drug transporters has now been well-characterized.[23] OAT1 plays a major role, along with OAT3, in the rate-limiting step of excretion of toxins and metabolites from the body into urine. It was determined that an OAT1 knockout resulted in reduced urinary concentration of XA in mice.[24] This indicates that OAT1 is responsible for the renal secretion of XA in mice. The OATs are considered to be important in the progression of chronic renal failure induced by nephrotoxicity.[25] Cisplatin significantly decreases renal OAT1 mRNA levels in male C57BL/6J mice.[26] Another study showed that aristolochic acid cause decreased expression of OAT1 and OAT3 in rats.[27] XA has been shown to act as a scavenger of peroxyl radicals *in vitro*.[28] Recently, Lima *et al.*[29] confirmed that XA proved to be a powerful antioxidant by inhibiting lipid peroxidation.

Propionylcarnitine (PLC) is a short-chain acyl derivative of L-carnitine (LC). Carnitine is an essential cofactor required for the translocation of activated long-chain fatty acids from extra mitochondrial coenzyme A into the inner mitochondrial matrix and then to intra mitochondrial coenzyme A.[30] This transport is essential to allow mitochondrial β-oxidation of long-chain fatty acids and thus to provide energy supply to the cells. Therefore, carnitine is an important factor in regulating substrate flux and energy balance across cell membranes, possibly preventing cell injury. Under normal physiological conditions, LC is highly conserved, because 90% of the filtered LC is reabsorbed by the renal tubule. A study indicated that the kidney is involved in the metabolism of PLC to LC. In addition, PLC has the potential not only to restore tissue carnitine stores but also to maintain membrane integrity,[31] which may account for the attenuation of oxidant stress. Aleisa *et al.*[32] reported that PLC could prevent the development of cisplatin-induced acute renal failure in rats by a mechanism related, at least in part, to the ability of PLC to increase intracellular carnitine content, with a consequent improvement in mitochondrial oxidative phosphorylation and energy production, as well as its ability to decrease oxidative stress. PLC is of value in preventing the decline of renal function that occurs during ischemia-reperfusion in models of syngeneic and allogeneic rat kidney transplantation, which possibly relates to lowering lipid peroxidation and free radical generation that eventually results in the preservation of tubular cell structure.[33,34] Many studies demonstrated that the accumulation of ROS is intimately associated with renal tubular cell injury and the process of renal calcium crystallization.[35–38] Mitochondria are major sources of intracellular ROS because they are sites of aerobic metabolism, and mitochondrial ROS production is increased under conditions of cell damage or increased stress. Niimi *et al.*[39] observed that the generation of ROS is induced via mitochondrial collapse in renal tubular cells exposed to calcium oxalate monohydrate crystals.

Sebacic acid and 3-hydroxysebacic acid (3-HS) are medium-chain dicarboxylic acids (DAs), which are derived from the ω-oxidation of fatty acids.[40–42] In addition, the β-oxidation of these acids takes place in both mitochondria and peroxisomes. Once in

*See online. https://www.jstage.jst.go.jp/article/jcbn/55/3/55_14-61/_article/supplement

doi: 10.3164/jcbn.14-61

the mitochondria, sebacic acid and 3-HS follow the same fate as free fatty acids, i.e., they are degraded to acetyl-CoA through β-oxidation. A previous study demonstrated that DAs consume carnitine when entering the mitochondria.[43]

In present study, the PLC level decreased in the CaOx group compared to the control group, this decrease was accompanied by increased levels of sebacic acid and 3-HS. This may imply a decline in fatty acid transport and decreased fatty acid β-oxidation, indicating that the perturbation of fatty metabolism has occurred. However, the level of PLC, sebacic acid and 3-HS was inversed in the XNA-treated group, which might indicate that XNA could protect renal tubular cells by maintaining fatty acid metabolism.

As is well known, DNA damage was a key feature of oxidative stress, and folic acid metabolism, purine metabolism, and pyrimidine metabolism were related to DNA injury and repair. In the CaOx group, p-aminobenzoic acid, 1,3-dimethyluracil, 7-methylguanine, and deoxyuridine monophosphate (dUMP) were decreased. In comparison, their levels in the XNA-treated group increased in various degrees. This implies that XNA could attenuate DNA injury.

In conclusion, we showed that a metabonomic strategy based on UPLC/Q-TOF has been developed to profile metabolic changes via calcium oxalate crystals in urine, and this allowed the evaluation of the anti-nephrolithiasis effect of XNA. Although the complex mechanism of calcium oxalate crystal deposition was not clearly elucidated, the present study might provide comprehensive insight regarding the metabolic response to TCM treatment in animal models.

Acknowledgments

This study was supported in part by grants from the National Scientific Foundation of China (81270773), TCM Supported Project (13401900105) and Basic science key Program (11JC1407902) from Science and Technology Commission of Shanghai Municipality and Scientific program from Changhai Hospital (CH125520301).

Conflict of Interest

No potential conflicts of interest were disclosed.

References

1 Scales CD Jr, Smith AC, Hanley JM, Saigal CS; Urologic Diseases in American Project. Prevalence of kidney stones in the United States. *Eur Urol* 2012; **62**: 160–165.
2 Edvardsson VO, Indridason OS, Haraldsson G, Kjartansson O, Palsson R. Temporal trends in the incidence of kidney stone disease. *Kidney Int* 2013; **83**: 146–152.
3 Khan SR. Is oxidative stress, a link between nephrolithiasis and obesity, hypertension, diabetes, chronic kidney disease, metabolic syndrome. *Urol Res* 2012; **40**: 95–112.
4 Rule AD, Bergstralh EJ, Melton LJ 3rd, Li X, Weaver AL, Lieske JC. Kidney stones and the risk for chronic kidney disease. *Clin J Am Soc Nephrol* 2009; **4**: 804–811.
5 Alexander RT, Hemmelgarn BR, Wiebe N, *et al*. Kidney stones and kidney function loss: a cohort study. *BMJ* 2012; **345**: e5287.
6 El-Zoghby ZM, Lieske JC, Foley RN, *et al*. Urolithiasis and the risk of ESRD. *Clin J Am Soc Nephrol* 2012; **7**: 1409–1415.
7 Ferraro PM, Taylor EN, Eisner BH, *et al*. History of kidney stones and the risk of coronary heart disease. *JAMA* 2013; **310**: 408–415.
8 Kim SH, Cho SK, Min TS, *et al*. Ameliorating effects of Mango (*Mangifera indica* L.) fruit on plasma ethanol level in a mouse model assessed with ^{1}H-NMR based metabolic profiling. *J Clin Biochem Nutr* 2011; **48**: 214–221.
9 Fukuhara K, Ohno A, Ota Y, *et al*. NMR-based metabonomics of urine in a mouse model of Alzheimer's disease: identification of oxidative stress biomarkers. *J Clin Biochem Nutr* 2013; **52**: 133–138.
10 Mi J, Duan J, Zhang J, Lu J, Wang H, Wang Z. Evaluation of antiurolithic effect and the possible mechanisms of Desmodium styracifolium and Pyrrosiae petiolosa in rats. *Urol Res* 2012; **40**: 151–161.
11 Tayefi-Nasrabadi H, Sadigh-Eteghad S, Aghdam Z. The effects of the hydroalcohol extract of Rosa canina L. fruit on experimentally nephrolithiasic Wistar rats. *Phytother Res* 2012; **26**: 78–85.
12 Yuliana ND, Khatib A, Link-Struensee AM, *et al*. Adenosine A1 receptor binding activity of methoxy flavonoids from Orthosiphon stamineus. *Planta Med* 2009; **75**: 132–136.
13 Zheng Q, Sun Z, Zhang X, *et al*. Clerodendranoic acid, a new phenolic acid from Clerodendranthus spicatus. *Molecules* 2012; **17**: 13656–13661.
14 Okada A, Nomura S, Higashibata Y, *et al*. Successful formation of calcium oxalate crystal deposition in mouse kidney by intraabdominal glyoxylate injection. *Urol Res* 2007; **35**: 89–99.
15 El-Tantawy WH, Mohamed SA, Abd Al Haleem EM. Evaluation of biochemical effects of Casuarina equisetifolia extract on gentamicin-induced nephrotoxicity and oxidative stress in rats. Phytochemical analysis. *J Clin Biochem Nutr* 2013; **53**: 158–165.
16 Zuo J, Khan A, Glenton PA, Khan SR. Effect of NADPH oxidase inhibition on the expression of kidney injury molecule and calcium oxalate crystal deposition in hydroxy-L-proline-induced hyperoxaluria in the male Sprague-Dawley rats. *Nephrol Dial Transplant* 2011; **26**: 1785–1796.
17 Lee HJ, Jeong SJ, Lee HJ, *et al*. 1,2,3,4,6-Penta-O-galloyl-beta-D-glucose reduces renal crystallization and oxidative stress in a hyperoxaluric rat model. *Kidney Int* 2011; **79**: 538–545.
18 Pawlak D, Tankiewicz A, Mysliwiec P, Buczko W. Tryptophan metabolism via the kynurenine pathway in experimental chronic renal failure. *Nephron* 2002; **90**: 328–335.
19 Xie G, Zheng X, Qi X, *et al*. Metabonomic evaluation of melamine-induced acute renal toxicity in rats. *J Proteome Res* 2010; **9**: 125–133.
20 Zhao YY. Metabonomics in chronic kidney disease. *Clin Chim Acta* 2013; **422**: 59–69.
21 Lenz EM, Bright J, Knight R, Wilson ID, Major H. A metabonomic investigation of the biochemical effects of mercuric chloride in the rat using 1H NMR and HPLC-TOF/MS: time dependent changes in the urinary profile of endogenous metabolites as a result of nephrotoxicity. *Analyst* 2004; **129**: 535–541.
22 Uwai Y, Honjo E. Transport of xanthurenic acid by rat/human organic anion transporters OAT1 and OAT3. *Biosci Biotechnol Biochem* 2013; **77**: 1517–1521.
23 Nigam SK, Bush KT, Bhatnagar V. Drug and toxicant handling by the OAT organic anion transporters in the kidney and other tissues. *Nat Clin Pract Nephrology* 2007; **3**: 443–448.
24 Wikoff WR, Nagle MA, Kouznetsova VL, Tsigelny IF, Nigam SK. Untargeted metabonomics identifies enterobiome metabolites and putative uremic toxins as substrates of organic anion transporter 1 (Oat1). *J Proteome Res* 2011; **10**: 2842–2851.
25 Enomoto A, Niwa T. Roles of organic anion transporters in the progression of chronic renal failure. *Ther Apher Dial* 2007; **11** Suppl 1: S27–S31.
26 Aleksunes LM, Augustine LM, Scheffer GL, Cherrington NJ, Manautou JE. Renal xenobiotic transporters are differentially expressed in mice following cisplatin treatment. *Toxicology* 2008; **250**: 82–88.
27 Lou Y, Li J, Lu Y, *et al*. Aristolochic acid-induced destruction of organic ion transporters and fatty acid metabolic disorder in the kidney of rats. *Toxicol Lett* 2011; **201**: 72–79.
28 Christen S, Peterhans E, Stocker R. Antioxidant activities of some tryptophan metabolites: possible implication for inflammatory diseases. *Proc Natl Acad Sci U S A* 1990; **87**: 2506–2510.
29 Lima VL, Dias F, Nunes RD, *et al*. The antioxidant role of xanthurenic acid in the Aedes aegypti midgut during digestion of a blood meal. *PLoS One* 2012; **7**: e38349.
30 Bremer J. Carnitine--metabolism and functions. *Physiol Rev* 1983; **63**: 1420–1480.
31 Tassani V, Cattapan F, Magnanimi L, Peschechera A. Anaplerotic effect of propionyl carnitine in rat heart mitochondria. *Biochem Biophys Res Commun* 1994; **199**: 949–953.
32 Aleisa AM, Al-Majed AA, Al-Yahya AA, *et al*. Reversal of cisplatin-induced carnitine deficiency and energy starvation by propionyl-L-carnitine

in rat kidney tissues. *Clin Exp Pharmacol Physiol* 2007; **34**: 1252–1259.
33 Mister M, Noris M, Szymczuk J, *et al*. Propionyl-L-carnitine prevents renal function deterioration due to ischemia/reperfusion. *Kidney Int* 2002; **61**: 1064–1078.
34 Azzollini N, Cugini D, Cassis P, *et al*. Propionyl-L-carnitine prevents early graft dysfunction in allogeneic rat kidney transplantation. *Kidney Int* 2008; **74**: 1420–1428.
35 Khan SR. Role of renal epithelial cells in the initiation of calcium oxalate stones. *Nephron Exp Nephrol* 2004; **98**: e55–e60.
36 Rashed T, Menon M, Thamilselvan S. Molecular mechanism of oxalate-induced free radical production and glutathione redox imbalance in renal epithelial cells: effect of antioxidants. *Am J Nephrol* 2004; **24**: 557–568.
37 Plotnikov EY, Kazachenko AV, Vyssokikh MY, *et al*. The role of mitochondria in oxidative and nitrosative stress during ischemia/reperfusion in the rat kidney. *Kidney Int* 2007; **72**: 1493–1502.
38 Khan SR. Reactive oxygen species as the molecular modulators of calcium oxalate kidney stone formation: evidence from clinical and experimental investigations. *J Urol* 2013; **189**: 803–811.
39 Niimi K, Yasui T, Hirose M, *et al*. Mitochondrial permeability transition pore opening induces the initial process of renal calcium crystallization. *Free Radic Biol Med* 2012; **52**: 1207–1217.
40 Verkade PE, Van Der. Researches on fat metabolism. II. *Biochem J* 1934; **28**: 31–40.
41 Kolattukudy PE, Walton TJ, Kushwaha RP. Biosynthesis of the C18 family of cutin acids: omega-hydroxyoleic acid, omega-hydroxy-9,10-epoxystearic acid, 9,10,18-trihydroxystearic acid, and their delta12-unsaturated analogs. *Biochemistry* 1973; **12**: 4488–4498.
42 Gregersen N, Mortensen PB, Kølvraa S. On the biologic origin of C6-C10-dicarboxylic and C6-C10-omega-1-hydroxy monocarboxylic acids in human and rat with acyl-CoA dehydrogenation deficiencies: *in vitro* studies on the omega- and omega-1-oxidation of medium-chain (C6-C12) fatty acids in human and rat liver. *Pediatr Res* 1983; **17**: 828–834.
43 Kølvraa S, Gregersen N. *In vitro* studies on the oxidation of medium-chain dicarboxylic acids in rat liver. *Biochim Biophys Acta* 1986; **876**: 515–525.

doi: 10.3164/jcbn.14-61